

Persistence of slow dynamics in $\text{Tb}(\text{OETAP})_2$ single molecule magnets embedded in conducting polymers

T.Orlando,^{1,2} M.Filibian,¹ S.Sanna,¹ N. Giménez-Agullo,³ C. Sáenz de Pipaón,³ P. Ballester,^{3,4} J.R. Galán-Mascarós,³ P.Carretta¹

¹ Department of Physics, University of Pavia-CNISM, I-27100 Pavia (Italy)

² Max Planck Institute for Biophysical Chemistry, D-37077 Gottingen (Germany)

³ Institute of Chemical Research of Catalonia (ICIQ), The Barcelona Institute of Science and Technology, E-43007 Tarragona (Spain)

⁴ Catalan Institution for Research and Advanced Studies (ICREA), Passeig Lluís Companys 23, E-08010, Barcelona (Spain)

E-mail: pietro.carretta@unipv.it

May 2016

Abstract.

The spin dynamics of $\text{Tb}(\text{OETAP})_2$ single ion magnets was investigated by means of muon spin resonance (μSR) both in the bulk material as well as when the system is embedded into PEDOT:PSS polymer conductor. The characteristic spin fluctuation time is characterized by a high temperature activated trend, with an energy barrier around 320 K, and by a low temperature tunneling regime. When the single ion magnet is embedded into the polymer the energy barrier only slightly decreases and the fluctuation time remains of the same order of magnitude even at low temperature. This finding shows that these single molecule magnets preserve their characteristics which, if combined with those of the conducting polymer, result in a hybrid material of potential interest for organic spintronics.

PACS numbers: 75.50.Xx, 76.75.+i, 74.50.Gb

1. Introduction

The trend towards ever-smaller electronic devices is driving electronics to its ultimate molecular-scale limit leading to severe drawbacks and to the breakdown of Moore's law [1] while, on the other hand, it allows for the exploitation of quantum effects both in electronics and in spintronics. Single Molecule Magnets (SMM) are among the most promising materials to be used in molecular spintronic devices [2, 3, 4] or as logic units in quantum computers [5], since they combine the classical macroscale properties of bulk magnetic materials with the advantages of nanoscale entities, such as quantum coherence. It has already been shown that molecular magnets can be used to build efficient memory devices and, in particular, single crystals can serve as

storage units for dynamic random access memory devices.[6] SMMs can be exploited for all these applications thanks to their bistability and sizeable energy barriers against magnetization reversal.[7] Nevertheless, most of SMMs are characterized by energy barriers in the tens of K range or below, giving rise to sufficiently long spin coherence times only at liquid helium temperature.[8] Accordingly, the study of lanthanide based single ion magnets (SIMs) where the crystal field (CF) splitting among the $|J, m\rangle$ states gives rise to energy barriers exceeding 700 K have attracted a great interest.[9, 10] These lanthanide-based single-ion magnets (SIMs) were discovered by Ishikawa and co-workers in a series of double-decker phthalocyanine (Pc) complexes.[9, 11, 12] Recently, other double decker (DD) SIMs [13] and triple-deckers,[14] have been synthesized, with a variety of ligands including polyoxometallates,[15] organometallic compounds,[16] and organic radicals.[17] However, all of them show energy barriers lower than the ones found in $\text{Ln}(\text{Pc})_2$ DD, in particular than the ones observed in $\text{Tb}(\text{Pc})_2$. Nowadays, one of the major challenges is to organize them in monolayers and to address them individually. $\text{Tb}(\text{Pc})_2$ has already been processed on graphite,[18] on carbon nanotubes [19] or on gold.[20] However, the poor solubility and stability in the gas phase of these DDs makes it difficult to obtain perfectly organized arrays from these SIMs. Thus, it would be a significant breakthrough if analogous magnetic properties could be found in easy to process single ion magnets.

Tetraazaporphyrins (or porphyrazines) are an attractive alternative for the bulkier Pc ligands. These macrocycles are constituted by four pyrrole rings bridged by azanitrogens, giving an analogous binding mode to Pc but without the extended aromatic skeleton. This, besides reducing the molecular size, causes an increase in the solubility and processability of their corresponding DD complexes. Recently we have reported the synthesis, structure and the basic magnetic properties of lanthanide DD complexes with octaethyltetraazaporphyrin (OETAP).[21] SIM behavior has been found in the Tb and Dy derivatives, as occurred with the related Pc analogs. Notably, in this case, the $\text{Ln}(\text{OETAP})_2$ neutral complexes are highly soluble in organic solvents and they can even be sublimed using mild conditions. Preliminary ^1H NMR measurements in $\text{Tb}(\text{OETAP})_2$ have allowed to evidence an energy barrier of a few hundreds of Kelvin degrees,[21] smaller than the one of $\text{Tb}(\text{Pc})_2$ but still sizeable and interesting for applications. Nevertheless, the shortening of the NMR relaxation rates lead to the suppression of the NMR signal over a broad temperature range, not allowing for an accurate study of the spin coherence time, one of the most relevant parameters for the technological applicability of SIMs. In order to suitably investigate the temperature dependence of the spin dynamics one can exploit the potential of muon spin resonance μSR technique. Here we show that the correlation time for the spin fluctuations in $\text{Tb}(\text{OETAP})_2$ SIMs is characterized by a high temperature activated behaviour followed by a low temperature tunneling regime. Moreover, we have investigated the behaviour of these SIMs when they are embedded in PEDOT:PSS conducting polymers representing an interesting system where the mutual interplay between the polymer transport properties and the SIMs magnetic state can be assessed. We found that the

temperature dependence of the correlation time for the spin fluctuations is very similar to the one of bulk $\text{Tb}(\text{OETAP})_2$, although with a slightly lower energy barrier, showing that these materials do preserve their SIM behaviour even when they are embedded into a conducting matrix.

2. Technical aspects and experimental results

$\text{Tb}(\text{OETAP})_2$ powders were grown and characterized as described in Ref.[21]. In order to embed the SIMs into the polymer the following synthesis procedure was adopted. Solid anhydrous 307 mg of PEDOT:PSS were added to 25 mL of HPLC grade dichloromethane and the resulting mixture was stirred for 4 days. Then 15.42 mg of $\text{Tb}(\text{OETAP})_2$ were added to the homogeneous suspension and stirred for 10 min. This solution was dropcast onto a Petri dish open to air, and the film formed through slow evaporation.

Zero field (ZF) and longitudinal field (LF) μSR measurements were carried out at the Paul Scherrer Institut (PSI) - Villigen (CH) by using Dolly and GPS instruments of the $S\mu\text{S}$ facility. In a μSR experiment a 100% spin-polarized beam of positive muons (μ^+) is implanted into the sample. The $1/2$ muon spin acts as a local magnetic probe and when a magnetic field B_μ perpendicular to the initial polarization is present, the muon spin precesses with an angular frequency $\omega_L = \gamma_\mu B_\mu$, where $\gamma_\mu = 2\pi \times 135.53 \text{ Mrad/s.T}$ is the muon gyromagnetic ratio.[22, 23] When the muon decays it emits a positron preferentially along its spin direction, allowing one to reconstruct the time evolution of the muon spin polarization or, equivalently, of the positron emission asymmetry $A(t)$. On the other hand, when a longitudinal field (LF) is applied along the initial muon polarization, no precession occurs and the time evolution of $A(t)$ is driven by static or dynamic relaxation mechanisms which are sensitive to the SIMs spin dynamics.[22, 23]

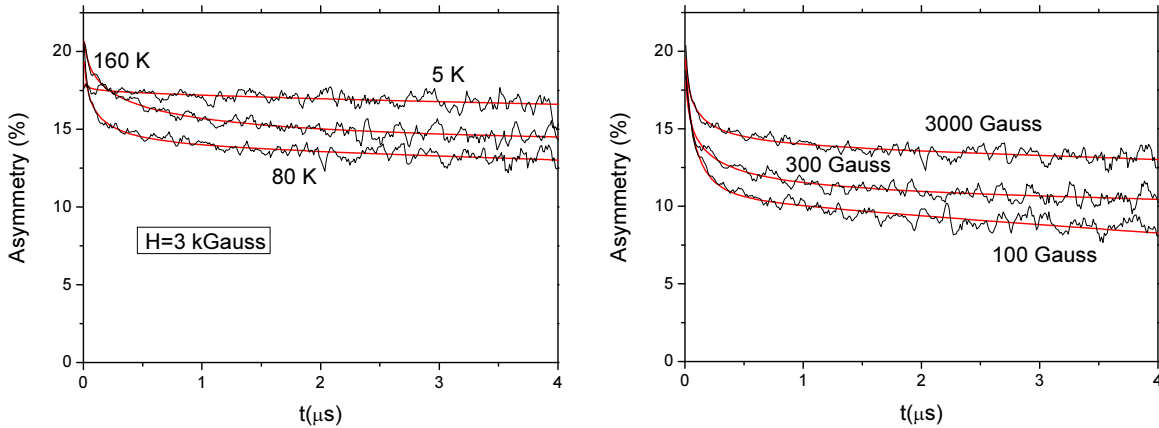


Figure 1. (left) Time evolution of the muon asymmetry in $\text{Tb}(\text{OETAP})_2$, in a LF of 3 kGauss, at three different temperatures. The solid lines are the best fits according to Eq.(1). (right) The asymmetry in the same sample is now shown, at $T = 80 \text{ K}$, for three different longitudinal fields.

Figure 1 shows the typical time evolution of the muon asymmetry in Tb(OETAP)₂ in LF geometry. One observes a very fast initial decay followed by a slow relaxation which indicates a distribution of relaxation rates, possibly associated with different muon implantation sites. As the temperature is lowered the relaxation gets faster and then, below about 80 K, the decay becomes significantly more stretched and the average rate decreases again. Accordingly, the asymmetry decay in Tb(OETAP)₂ can suitably be fit as the sum of two components

$$A(t) = A_1 e^{-(\lambda_F t)^\beta} + A_2 e^{-\lambda t} + Bck, \quad (1)$$

with $\lambda_F \gg \lambda$ the corresponding relaxation rates, β a stretching exponent and Bck a small constant term accounting for the sample environment background. Owing to the very fast initial relaxation the estimate of λ_F is characterized by large errors, even by fixing the amplitude of A_1 and A_2 as temperature independent. For this reason we have rather concentrated on the temperature dependence of the slow relaxing component relaxation rate λ . One notices a clear maximum around 80 K for the measurements performed at different magnetic fields (see Fig.3). Moreover, it is observed that upon increasing the field intensity the asymmetry decay gets progressively slower. Although this behaviour is considered often as an evidence of a static field distribution[22, 23], here it is not the case. In fact, relaxation rates of the order of a few μs^{-1} arising from a static field distribution should be completely quenched in a magnetic field of 1 kGauss, while they are not (see Fig. 1). This indicates that the LF relaxation is determined by the spectral density of the spin fluctuations at ω_L , which is varied by changing the magnetic field intensity.[23]

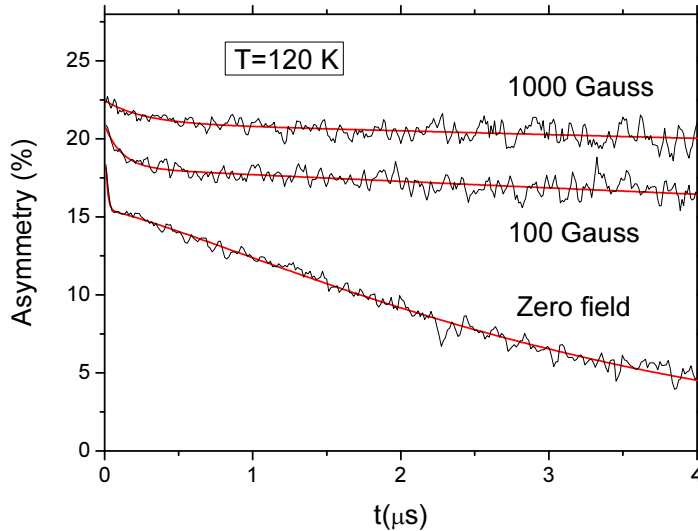


Figure 2. Time evolution of the muon asymmetry in Tb(OETAP)₂PEDOT:PSS, at $T = 120$ K, for three different longitudinal fields and in ZF. The solid lines, in LF, are the best fits according to Eq.(2) in the text, while for the fit of the ZF data a gaussian decay was added to Eq.(2).

At $H = 3$ kGauss the asymmetry decay could also be fit reasonably well, even if

with a slightly lower accuracy, with a single stretched exponential decay

$$A(t) = A_s e^{-(\lambda_s t)^\beta} + B c k_s . \quad (2)$$

Even if $\lambda_s \gg \lambda$ their temperature dependence is rather similar, as well as the temperature dependence of the characteristic spin fluctuation time derived from them (Fig. 4), as we shall see in the following.

The asymmetry decay in Tb(OETAP)₂PEDOT:PSS shows a clearly different behaviour in zero-field. In fact, as it is shown in Fig.2 in ZF the asymmetry is characterized by a very fast initial decay followed by a gaussian-like relaxation. This second contribution is likely due to the dipolar fields generated by ¹H nuclei in the PEDOT:PSS polymer. In fact, this second term is quenched in a 100 Gauss magnetic field. At those field magnitude or at larger field intensities the data could be fit by Eq. 2. The temperature dependence of λ_s for Tb(OETAP)₂PEDOT:PSS is shown in Fig. 3. Similarly to Tb(OETAP)₂, also here one notices a maximum around 80 K.

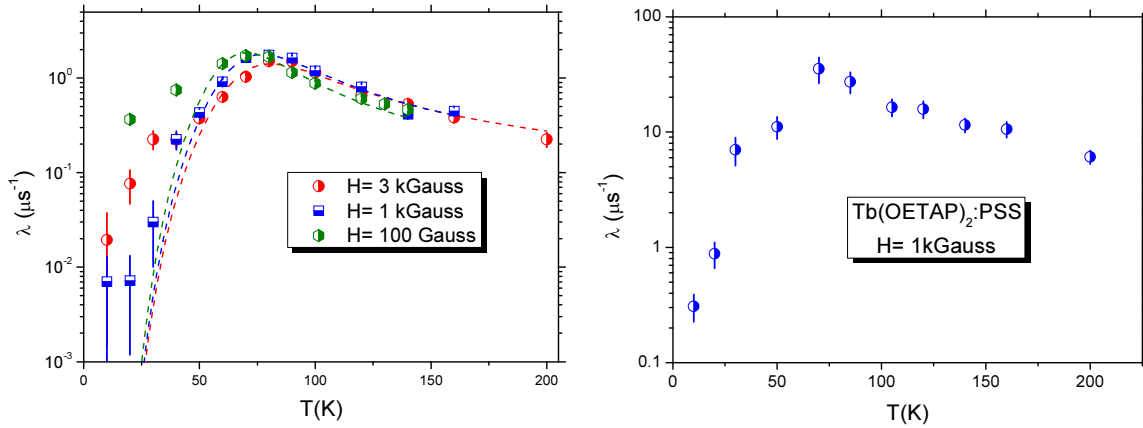


Figure 3. (left) Temperature dependence of the LF decay rate λ in Tb(OETAP)₂ at three different longitudinal fields. The dashed lines are the best fits according to Eq.(6) in the text. (right) Temperature dependence of λ_s in Tb(OETAP)₂PEDOT:PSS for $H = 1$ kGauss.

3. Discussion

Ln-based SIMs are characterized by an anisotropy barrier determined by the crystal field (CF) splitting. Since the energy difference between the muon hyperfine levels and the $|J, m\rangle$ CF levels of Tb³⁺ spin is large, the muon longitudinal relaxation rate λ is driven by an indirect relaxation mechanism involving a muon spin flip without a change in m . This can occur thanks to the tensorial nature of the dipolar hyperfine coupling constant, which allows the coupling of the transverse components of the local field $h_{x,y}$ at the muon to J_z . Thus, denoting with (τ_m) the finite life-time of the crystal field levels

induced mainly by spin-phonon scattering processes, λ can be written in the form[24]

$$\lambda = \frac{\gamma_\mu^2 \langle \Delta h_\perp^2 \rangle}{Z} \sum_{m=-6}^{+6} \frac{\tau_m e^{-E_m/T}}{1 + \omega_L^2 \tau_m^2} \quad , \quad (3)$$

E_m being the eigenvalues of the CF levels and Z the corresponding partition function. It is noted that the low magnetic field (of the order of 1000 Gauss) applied during μ SR experiments yield a negligible correction to E_m and, hence, its effect can be disregarded for $k_B T \gg \mu_B H J \sim 1$ K. The life-time for the m levels can be expressed in terms of the transition probabilities $p_{m,m\pm 1}$ between m and $m \pm 1$ levels, which depend on the CF eigenvalues and on the spin-phonon coupling constant C [25]:

$$\frac{1}{\tau_m} = p_{m,m-1} + p_{m,m+1} \quad , \quad (4)$$

$$p_{m,m\pm 1} = C \frac{(E_{m\pm 1} - E_m)^3}{e^{(E_{m\pm 1} - E_m)/T} - 1} \quad (5)$$

Since the CF splitting between the lowest levels of Tb^{3+} is likely larger than the thermal energy, as it will be confirmed in the following, one can to a first approximation cut the summation in Eq. 3 to the first term so that one can write

$$\lambda = \gamma_\mu^2 \langle \Delta h_\perp^2 \rangle \frac{\tau_c}{1 + \omega_L^2 \tau_c^2} \quad , \quad (6)$$

with $\tau_c = (1/C\Delta E^3) \exp(\Delta E/T)$, where ΔE is the CF splitting between the lowest $m = \pm 6$ and $m = \pm 5$ levels. Notice that although a large crystal field splitting yields a decrease in the fluctuations owing to the Boltzmann exponential factor, it also implies a large spin-phonon coupling so that at the end one finds a non-exponential dependence of the dynamics on the anisotropy barrier. If now one fits λ data of $\text{Tb}(\text{OETAP})_2$ in Fig.3 with Eq.6, taking for τ_c the activated T -dependence reported above, one observes that the data follow reasonably well the expected trend down to 60-50 K while clear deviations are found at lower temperature. Hence, at least down to 60 K τ_c shows an activated behaviour with an energy barrier determined by the crystal field splitting. The failure of the fit at low temperature clearly indicates a deviation of τ_c from the activated trend. In order to derive the temperature dependence of τ_c from $\lambda(T)$ data, we inverted Eq.6 obtaining

$$\tau_c = \frac{1}{\lambda \omega_L} \left(\lambda_{max} \pm \sqrt{\lambda_{max}^2 - \lambda^2} \right) \quad , \quad (7)$$

with λ_{max} the maximum value of $\lambda(T)$, achieved for $\omega_L \tau_c = 1$. Notice that out of the two solutions just one is physically meaningful, i.e. the one yielding τ_c increasing on decreasing temperature. The temperature dependence of τ_c derived from Eq.7 is shown in Fig.4.

By plotting τ_c vs $1000/T$ in a semi-log scale one notices a high temperature linear trend, namely an activated trend of τ_c , and then a low temperature flattening which should be associated with the tunneling among the low-lying energy levels. In particular, one can write that

$$\frac{1}{\tau_c} = \frac{1}{\tau_{tunn}} + \frac{e^{-\Delta E/T}}{C\Delta E^3} \quad , \quad (8)$$

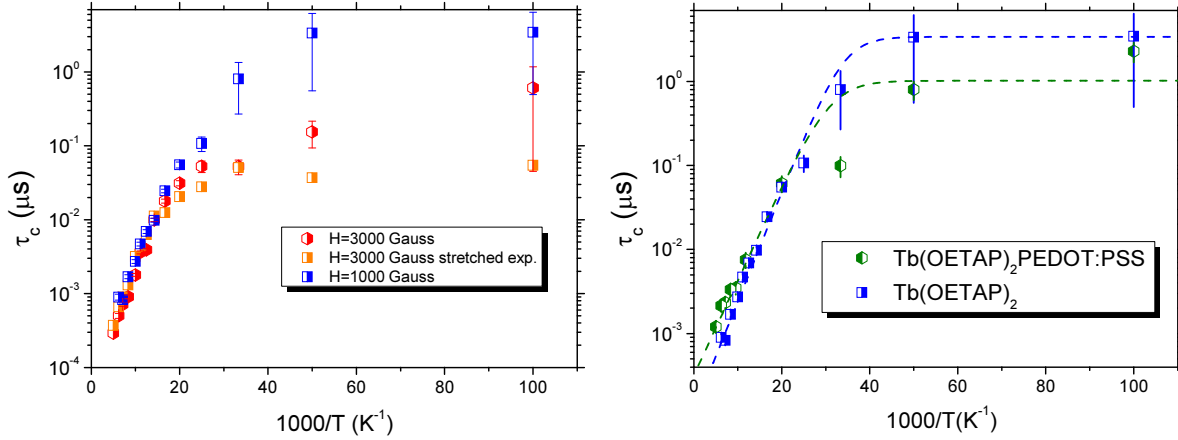


Figure 4. (left) The correlation time for the spin fluctuations in $\text{Tb}(\text{OETAP})_2$, for different magnetic field intensities, is reported as a function of $1000/T$. (right) Comparison of the correlation times of bulk $\text{Tb}(\text{OETAP})_2$ with that of $\text{Tb}(\text{OETAP})_2$ embedded in the polymeric matrix as a function of $1000/T$. The dashed line shows the behaviour according to Eq. 8, as described in the text.

with $1/\tau_{\text{tunn}}$ the tunneling rate. The high temperature data for the different magnetic fields can be fit with the same activation energy $\Delta E = 320 \pm 20$ K and spin-phonon coupling constant $C = 250 \pm 30$ Hz/ K^3 , a value somewhat smaller than the one found in LnPc_2 compounds [10]. On the other hand, the low temperature behaviour depends on the magnetic field and on the asymmetry fitting procedure. The dependence on the fitting law stems from the fact that at low temperature the very fast initial decay gives rise to a large uncertainty in the relaxation rate when it is fit with the stretched exponential law.

If now we turn to the behaviour of the correlation time for the $\text{Tb}(\text{OETAP})_2$ spin fluctuations when it is embedded in the PEDOT:PSS conducting polymers one notices that the correlation time shows a behaviour very similar to the one found in bulk $\text{Tb}(\text{OETAP})_2$ even if with a slightly lower activation energy $\Delta E = 260 \pm 30$ K with a spin phonon coupling constant $C = 180 \pm 30$ Hz/ K^3 . Remarkably in both materials the fluctuation time becomes longer than a μs at temperatures of the order of a few tens of Kelvin degree, making those materials potentially interesting for future applications.

4. Conclusion

From a series of LF μSR experiments we have shown that $\text{Tb}(\text{OETAP})_2$ is characterized by a high temperature activated dynamics with a correlation time increasing above the μs already at temperatures of a few tens of K. At low temperature the tunneling processes among the two fold degenerate ground-state dominate the spin fluctuations and a clear flattening of the correlation time is noticed. μSR measurements performed in $\text{Tb}(\text{OETAP})_2$ molecules show that the spin dynamics is only weakly affected by the

conducting polymers suggesting that these hybrid materials are potentially interesting for the development of organic spintronics.

Acknowledgements

Hubertus Luetkens and Alex Amato are gratefully acknowledged for their help during the μ SR measurements at PSI. We acknowledge financial support from the European Union EU (ERC Stg grant 279313, CHEMCOMP), the Spanish Ministerio de Economía y Competitividad (MINECO, project CTQ2015-71287-R and the Severo Ochoa Excellence Accreditation 20142018 (SEV-2013-0319), the Generalitat de Catalunya (2014 SGR 797) and the ICIQ Foundation.

References

- [1] Waldrop M M 2016 *Nature* **530** 145
- [2] Gatteschi D, Sessoli R and Villain J 2007 in *Molecular Nanomagnets*, Oxford University Press, Oxford.
- [3] Bogani L and Wernsdorfer W 2008 *Nature Mat.* **7** 179
- [4] Ardavan A, Rival O, Morton J J L, Blundell S J, Tyryshkin A M, Timco G A, Winpenny R E P 2007 *Phys. Rev. Lett.* **98** 057201
- [5] Leuenberger M N and Loss D 2001 *Nature* **410** 789
- [6] Ekert A K and Jozsa R 1996 *Rev. Mod. Phys.* **68** 733
- [7] Branzoli F, Carretta P, Filibian M, Zoppellaro G, Graf M J, Galan-Mascarós J R, Fuhr O, Brink S and Ruben M 2009 *J. Am. Chem. Soc.* **131** 4387
- [8] Milios C J, Vinslava A, Wernsdorfer W, Moggach S, Parsons S, Perlepes S P, Christou G and Brechin E K 2007 *J. Am. Chem. Soc.* **129** 2754
- [9] Ishikawa N, Sugita M, Ishikawa T, Koshihara S and Kaizu Y 2005 *J. Phys. Chem. B* **108** 11265
- [10] Branzoli F, Carretta P, Filibian M, Graf M J, Klyatskaya S, Ruben M, Coneri F and Dhakal P 2010 *Phys. Rev. B* **82** 134401
- [11] Ishikawa N, Sugita M, Tanaka T, Ishikawa T, Koshihara S and Kaizu Y 2004 *Inorg. Chem.* **43** 5498
- [12] Ishikawa N, Mizuno Y, Takamatsu S, Ishikawa T and Koshihara S 2008 *Inorg. Chem.* **47** 10217
- [13] Wang H, Qian K, Wang K, Bian Y, Jiang J and Gao S 2011 *Chem. Comm.* **47** 9624
- [14] Katoh K, Kajiwarra T, Nakano M, Nakazawa Y, Wernsdorfer W, Ishikawa N, Breedlove B K and Yamashita M 2011 *Chem. Eur. J.* **17** 117
- [15] Aldamen M, Clemente-Juan J M, Coronado E, Martí-Gastaldo C and Gaita-Arino A 2008 *J. Am. Chem. Soc.* **130** 8874
- [16] Tuna F, Smith C A, Bodensteiner M, Ungur L, Chibotaru L F, McInnes E J L, Winpenny R E P, Collison D and Layfield R A 2012 *Angew. Chem. Int. Ed.* **51** 6976
- [17] Lopez N, Prosvirin A V, Zhao H, Wernsdorfer W and Dunbar K R 2009 *Chem. Eur. J.* **15** 11390
- [18] Gonidec M, Biagi R, Corradini V, Moro F, De Renzi V, del Pennino U, Summa D, Muccioli L, Zannoni C, Amabilino D B and Veciana J 2011 *J. Am. Chem. Soc.* **133** 6603
- [19] Klyatskaya S, Galán-Mascarós J R, Bogani L, Hennrich F, Kappes M, Wernsdorfer W and Ruben M 2009 *J. Am. Chem. Soc.* **131** 15143
- [20] Katoh K, Yoshida Y, Yamashita M, Miyasaka H, Breedlove B K, Kajiwarra T, Takaishi S, Ishikawa N, Ishiki H, Zhang Y F, Komeda T, Yamagishi M and Takeya J 2009 *J. Am. Chem. Soc.* **131** 9967

- [21] Giménez-Agulló N, Sáenz de Pipaón C, Adriaenssens L, Filibian M, Martínez-Belmonte M, Escudero-Adán E C, Carretta P, Ballester P and Galán-Mascarós J R 2014 *Chem. Eur. J.* **20** 12817
- [22] Blundell S J 1999 *Contemp. Phys.* **40** 175
- [23] Yaouanc A and Dalmas de Réotier P 2011 in *Muon Spin Rotation, Relaxation, and Resonance: Applications to Condensed Matter* Oxford University Press, Oxford
- [24] Lascialfari A, Jang Z H, Borsa F, Carretta P and Gatteschi D 1998 *Phys. Rev. Lett.* **81** 3773
- [25] Villain J, Hartmann-Boutron F, Sessoli R and Rettori A 1994 *Europhys. Lett.* **27** 159